

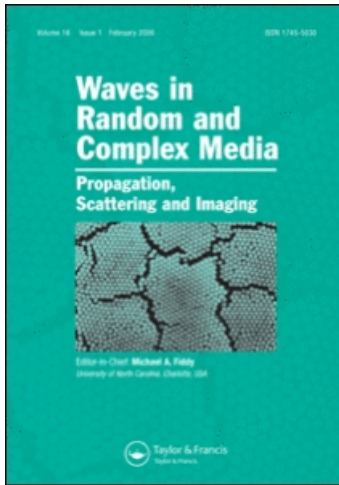
This article was downloaded by: [University of Liverpool]

On: 20 August 2008

Access details: Access Details: [subscription number 773559798]

Publisher Taylor & Francis

Informa Ltd Registered in England and Wales Registered Number: 1072954 Registered office: Mortimer House, 37-41 Mortimer Street, London W1T 3JH, UK



Waves in Random and Complex Media

Publication details, including instructions for authors and subscription information:

<http://www.informaworld.com/smpp/title-content=t716100762>

Swiss roll lattices: numerical and asymptotic modeling

F. Zolla ^a; A. Nicolet ^b; S. Guenneau ^c

^a UMR CNRS 6133, Faculté de Saint Jérôme case 162, Université de Provence, Marseille Cedex 20, France

^b UMR CNRS 6133, Faculté de Saint Jérôme case 162, Université Paul Cézanne, Marseille Cedex 20, France

^c UMR CNRS 6133, Faculté de Saint Jérôme case 162, C.N.R.S. Institut Fresnel, Marseille Cedex 20, France

Online Publication Date: 01 November 2007

To cite this Article Zolla, F., Nicolet, A. and Guenneau, S.(2007)'Swiss roll lattices: numerical and asymptotic modeling',Waves in Random and Complex Media,17:4,571 — 579

To link to this Article: DOI: 10.1080/17455030701504350

URL: <http://dx.doi.org/10.1080/17455030701504350>

PLEASE SCROLL DOWN FOR ARTICLE

Full terms and conditions of use: <http://www.informaworld.com/terms-and-conditions-of-access.pdf>

This article may be used for research, teaching and private study purposes. Any substantial or systematic reproduction, re-distribution, re-selling, loan or sub-licensing, systematic supply or distribution in any form to anyone is expressly forbidden.

The publisher does not give any warranty express or implied or make any representation that the contents will be complete or accurate or up to date. The accuracy of any instructions, formulae and drug doses should be independently verified with primary sources. The publisher shall not be liable for any loss, actions, claims, proceedings, demand or costs or damages whatsoever or howsoever caused arising directly or indirectly in connection with or arising out of the use of this material.

Swiss roll lattices: numerical and asymptotic modeling

F. ZOLLA[†], A. NICOLET^{‡*} and S. GUENNEAU[§]

[†]Université de Provence, [‡]Université Paul Cézanne, [§]C.N.R.S. Institut Fresnel, UMR CNRS 6133, Faculté de Saint Jérôme case 162, 13397 Marseille Cedex 20, France

(Received 15 February 2007; in final form 29 May 2007)

The design of metamaterials for microwave devices with new properties is an active field of research. Various kinds of structures such as the ‘Swiss roll’ are proposed as candidates with innovative properties. In order to model such structures, we consider the out-of-plane propagation of electromagnetic waves in a lattice with arbitrary dielectric or perfectly conducting inclusions. The problem is reduced to finding Bloch modes characterized by a transverse Bloch propagation vector, a longitudinal propagation constant, and a pulsation. The dispersion curves obtained give the relevant information on the physical properties of the equivalent material. Eventually, an asymptotic approach is given which allows us not only to foresee the first dispersion curves but also to determine precisely enough the main characteristics of the map of the corresponding modes.

1. Introduction

In this paper, we consider the out-of-plane propagation of electromagnetic waves in lattices with Swiss roll inclusions. The problem is reduced to finding Bloch modes characterized by a transverse Bloch propagation vector \mathbf{k}_T , a longitudinal propagation constant β , and a pulsation ω . These modes also have to satisfy both the Maxwell equations and the Floquet–Bloch theorem. Because of the non-vanishing β , a full wavevector model involving the three components of the electric field (or magnetic field) is necessary. The numerical model is a finite element method (edge elements for the transverse component and node elements for the longitudinal component) together with Bloch boundary conditions [1]. Given $\mathbf{k} = (\mathbf{k}_T, \beta)$, a numerical matrix eigenvalue problem is solved to find the corresponding ω 's.

2. Periodic waveguides

We consider a structure invariant along the z -axis and also periodic in the xy -plane, as shown in figure 1.

2.1 Invariance along the z -axis: Propagation

Choosing a time dependence in $e^{-i\omega t}$, and taking into account the invariance of the guide along its z -axis, we define time-harmonic two-dimensional electric and magnetic fields \mathbf{E} and

*Corresponding author. E-mail: andre.nicolet@fresnel.fr

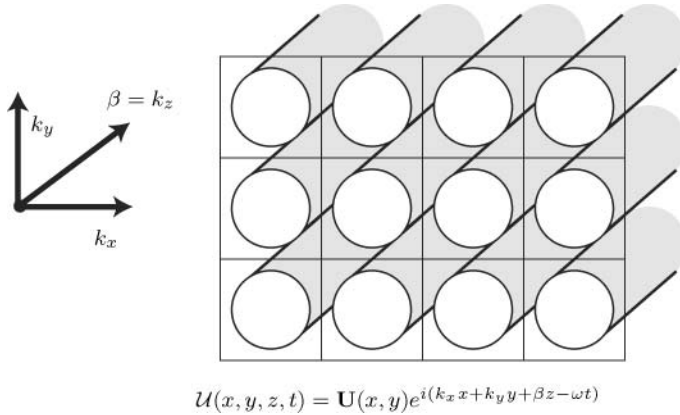


Figure 1. A system with a continuous translational invariance along the z -axis together with a two-dimensional periodicity in the xy -plane and the general form of propagating Bloch modes $\mathcal{U}(x, y, z, t)$, $\mathbf{U}(x, y)$ being a periodic function.

H by:

$$\begin{aligned}\mathcal{E}(x, y, z, t) &= \Re(\mathbf{E}(x, y) e^{-i(\omega t - \beta z)}) \\ \mathcal{H}(x, y, z, t) &= \Re(\mathbf{H}(x, y) e^{-i(\omega t - \beta z)})\end{aligned}\quad (2.1)$$

where ω is the angular frequency and β is the propagating constant of the guided mode (β is supposed to be a non-negative real number). Note that \mathbf{E} and \mathbf{H} are complex valued fields depending on two variables (coordinates x and y) but still with three components (along the three axes). Moreover, the following operator is used in the sequel:

$$\text{curl}_\beta \mathbf{U}(x, y) = \text{curl}(\mathbf{U}(x, y) e^{i\beta z}) e^{-i\beta z}. \quad (2.2)$$

2.2 Periodicity in the xy -plane: Floquet–Bloch theory

Given two linearly independent vectors \mathbf{a} and \mathbf{b} in the xy -plane, the set of points $\{n\mathbf{a} + m\mathbf{b}, n, m \in \mathbb{Z}\}$ is called the lattice. The primitive cell Y is a subset of \mathbb{R}^2 such that for any point \mathbf{r}' of \mathbb{R}^2 there exist unique $\mathbf{r} = x\mathbf{e}_x + y\mathbf{e}_y \in Y$ and $n, m \in \mathbb{Z}$ such that $\mathbf{r}' = \mathbf{r} + n\mathbf{a} + m\mathbf{b}$, as shown in figure 2(a). A function $U(\mathbf{r})$ is Y -periodic if $U(\mathbf{r} + n\mathbf{a} + m\mathbf{b}) = U(\mathbf{r})$ for any $n, m \in \mathbb{Z}$.

The waveguide is Y -periodic if $\varepsilon_r(x, y)$ and $\mu_r(x, y)$ are Y -periodic functions. The problem reduces then to looking for Bloch wave solutions $\mathbf{U}_{\mathbf{k}_T}$ that have the form:

$$\mathbf{U}_{\mathbf{k}_T}(\mathbf{r}) = e^{i\mathbf{k}_T \cdot \mathbf{r}} \mathbf{U}(\mathbf{r}) = e^{i(k_x x + k_y y)} \mathbf{U}(x, y), \quad \forall (x, y) \text{ in } \mathbb{R}^2 \quad (2.3)$$

where $\mathbf{U}(x, y)$ is a Y -periodic function and $\mathbf{k}_T = k_x \mathbf{e}_x + k_y \mathbf{e}_y \in Y^* \subset \mathbb{R}^2$ is a parameter (the Bloch vector or quasi-momentum in solid state physics). $Y^* \subset \mathbb{R}^2$ is the dual cell (first Brillouin zone), i.e. the primitive cell of the reciprocal lattice determined by the two vectors \mathbf{a}^* and \mathbf{b}^* such that $\mathbf{a}^* \cdot \mathbf{a} = 2\pi$, $\mathbf{a}^* \cdot \mathbf{b} = 0$, $\mathbf{b}^* \cdot \mathbf{a} = 0$, $\mathbf{b}^* \cdot \mathbf{b} = 2\pi$, as shown in figure 2(b). Such solutions $\mathbf{U}_{\mathbf{k}_T}$ are said to be (\mathbf{k}_T, Y) -periodic in the sequel (though they are not periodic but almost-periodic). The pair $(\mathbf{E}_{\mathbf{k}_T}, \mathbf{H}_{\mathbf{k}_T})$ associated with the Bloch vector \mathbf{k}_T is called an

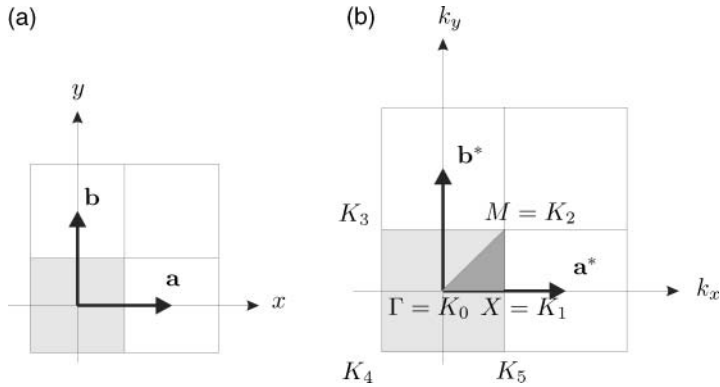


Figure 2. An example of a two-dimensional periodic structure (the basic cell is a square with a side length Δ): a representation of some lattice cells with the lattice vectors $\mathbf{a} = \Delta \mathbf{e}_x$ and $\mathbf{b} = \Delta \mathbf{e}_y$ (a) and a representation of some cells of the reciprocal lattice with the lattice vectors $\mathbf{a}^* = \frac{2\pi}{\Delta} \mathbf{e}_x$ and $\mathbf{b}^* = \frac{2\pi}{\Delta} \mathbf{e}_y$ (b).

electromagnetic propagating Bloch mode if $\mathbf{E}_{\mathbf{k}_T}$ and $\mathbf{H}_{\mathbf{k}_T}$ are (\mathbf{k}_T, Y) -periodic fields satisfying the spectral problem:

$$\begin{aligned} \varepsilon_r(x, y)^{-1} \operatorname{curl}_\beta \mathbf{H}_{\mathbf{k}_T} &= -i\omega \varepsilon_0 \mathbf{E}_{\mathbf{k}_T} \\ \mu_r(x, y)^{-1} \operatorname{curl}_\beta \mathbf{E}_{\mathbf{k}_T} &= i\omega \mu_0 \mathbf{H}_{\mathbf{k}_T} \end{aligned} \quad (2.4)$$

with $(\omega, \mathbf{k}_T) \in \mathbb{R}_+ \times Y^*$ and $(\mathbf{E}_{\mathbf{k}_T}, \mathbf{H}_{\mathbf{k}_T}) \neq (\mathbf{0}, \mathbf{0})$. The point is that any solution of Maxwell's equations in the considered periodic structure can be expressed in terms of linear combinations of Bloch waves (Bloch theorem, see e.g. [1]).

2.3 Finite elements

The finite element formulation is completely identical to the non-periodic one for waveguides: it is a full wave model where the electric field $\mathbf{E}_{\mathbf{k}_T}$ is the unknown, with edge elements for the transverse component and node elements for the longitudinal component [1, 3, 4]. The study is now reduced to the primitive cell Y which is meshed and in which the integrations are performed. Some technique must be found to ensure that the solution is a (\mathbf{k}_T, Y) -periodic Bloch mode. This can be imposed by using special boundary conditions as explained in [1, 3].

3. Geometry of Swiss rolls

In this paper, we only deal with Swiss rolls as ideal structures which can be considered as infinitely thin sheets made of perfectly conducting metal and therefore these ideal structures can be represented by a curved line where the tangential electric field is forced to zero. The aforementioned curved lines are built as a juxtaposition of quarters of circles ($\mathcal{C}_1, \mathcal{C}_2, \dots, \mathcal{C}_N$, in figure 3) of different radii and different centers (four in our model) in such a way that the curved line Γ is a spiral of class C^1 .

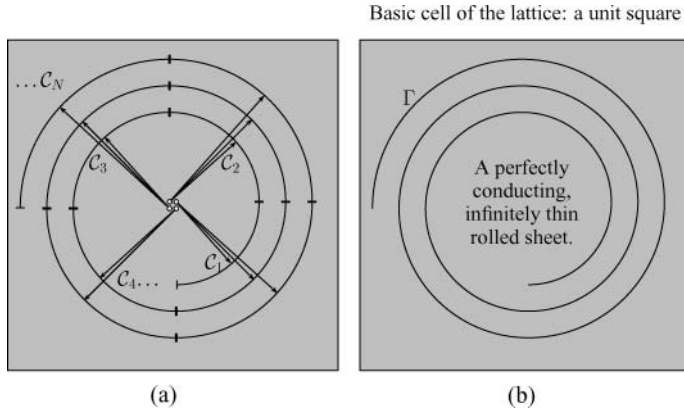


Figure 3. Swiss rolls: A perfectly conducting, infinitely thin rolled sheet within a dielectric bulk with $\epsilon_r = 1$, and $\mu_r = 1$. (a) The Swiss rolls are considered as a juxtaposition of quarters of circle. The radii and the centers (four in our model) of these quarters of circle are chosen in such a way that the spiral Γ is of class C^1 . (b) The Swiss rolls are ideal structures; both infinitely thin and made of perfectly conducting metal.

4. A square lattice of Swiss rolls

In this paragraph, some results concerning lattices of Swiss rolls are presented. The structure considered here is a unit square lattice (the Brillouin zone is then a square with a side length equal to 2π) with inclusions that are wrapped metallic sheets (figure 3).

Figure 4 shows an example of dispersion curves for some conical incidence. Although the structure is not strictly isotropic we disregard this fact and consider the irreducible Brillouin zone of a circular inclusion. This is only for the sake of simplicity of the graphical

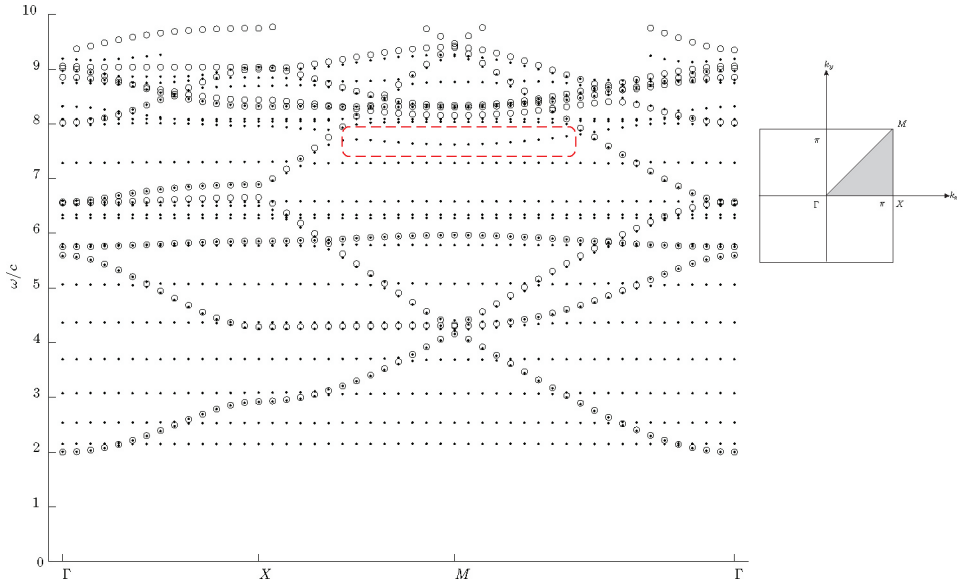


Figure 4. Band diagram of a triple loop Swiss roll lattice for $\beta = 2 \text{ m}^{-1}$ versus $\frac{\omega}{c}$ on the boundary of the irreducible Brillouin zone depicted by the points \cdot together with the propagating modes corresponding to the ‘obstructed’ Swiss roll depicted by the points \circ . Note that although the obstructed Swiss rolls were a good approximation for the propagative modes, some significant discrepancies may appear. See, for instance, the points within the dashed box. As a result, band diagrams have to be computed accurately enough.

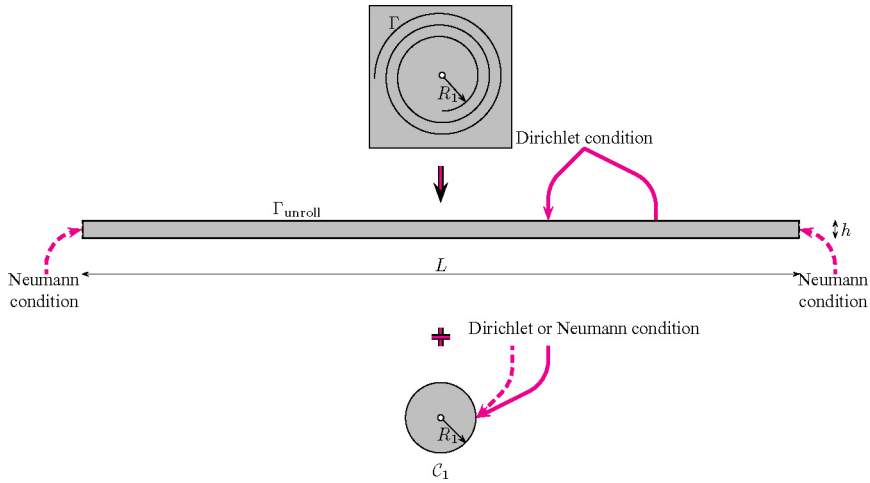


Figure 5. A twisted sheet is unrolled to an equivalent rectangular waveguide.

representations. Moreover, for the sake of clarity, in our numerical experiments, we only deal with $\varepsilon_r = 1$ and $\mu_r = 1$. The most striking fact are the almost perfectly flat lines crossing the diagram. In order to understand their origin, the dispersion diagram is first compared with the dispersion diagram of closed cylinders: the outer boundary is the same as the one of the open Swiss roll but the outer opening is closed by a perfectly conducting segment so that the electromagnetic field is considered only in the interstitial space between the cylinders. It appears that this diagram matches more or less the curved parts of the Swiss roll diagram (figure 4). This suggests that the remaining curves correspond to localized modes ‘inside’ the rolls i.e. inside the interstices of the Swiss roll or within the interior cavity (see figure 5).

5. Computation of internal localized modes

5.1 Interstitial localized modes

To confirm the hypothesis made above, these interstitial localized propagation are computed. For such a mode, the curvature of the roll is probably negligible and, in order to obtain an analytical estimation, the structure is unrolled (figure 5) to an equivalent rectangular waveguide (length L , height $h \ll L$) with perfectly conducting boundaries on the long sides (homogeneous Dirichlet condition) and no current on the small sides (homogeneous Neumann condition). The eigenfrequencies for propagating modes in such a structure are given by:

$$k_{0,n,m}^2 = \left(\beta^2 + m^2 \frac{\pi^2}{L^2} + n^2 \frac{\pi^2}{h^2} \right) / \varepsilon_r \quad m, n \in \mathbb{N}$$

where ε_r is the relative permittivity inside the interstices of the Swiss roll. As h is much smaller than L , the lower frequencies correspond to $n = 0$ and are indexed by m and therefore the corresponding normalized eigenfrequencies are approximately given by

$$k_{0,m} = \sqrt{\left(\beta^2 + m^2 \frac{\pi^2}{L^2} \right) / \varepsilon_r}$$

Figure 6 and table 1 show that this is obviously a good estimation for the flat curves.

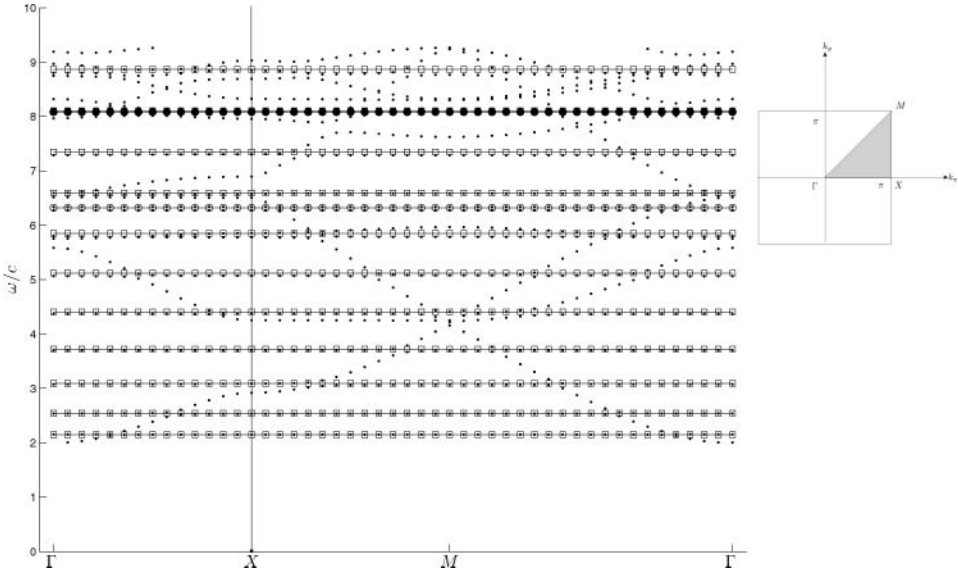


Figure 6. Band diagram of a three loop Swiss roll lattice for $\beta = 2 \text{ m}^{-1}$ versus $\frac{\omega}{c}$ on the boundary of the irreducible Brillouin zone depicted by the points ‘ \cdot ’ together with the localized modes depicted by the straight-lines ‘ \square ’ (Interstitial localized modes), ‘ \circ ’ (internal localized T.E. modes) and ‘ \bullet ’ (internal T.M. localized modes).

5.2 Internal localized modes

The second kind of localized modes concerns the modes which are concentrated within the core of the Swiss roll. Once again, in order to obtain estimations in closed form, we assume that the core of the Swiss roll is pretty well approximated by a closed circular cavity, the radius of this circular cavity being the mean radius R_{int} of the four most internal quarters of circle ($\mathcal{C}_1, \mathcal{C}_2, \mathcal{C}_3$ and \mathcal{C}_4 on figure 3a). The computation of the constants of propagation associated with such modes is well known and depends on the polarization and are linked with the zeroes of Bessel functions, namely:

$$J'_n(\kappa_{n,m} R_{\text{int}}) = 0 \quad (\text{T.E. modes}) \quad J_n(\kappa_{n,m} R_{\text{int}}) = 0 \quad (\text{T.M. modes}),$$

Table 1. Detail for the first 23 modes for a Bloch vector $\mathbf{k}_{\Gamma} = \pi \mathbf{e}^x + 2\mathbf{e}^z$ (corresponding to the point X). The points (\cdot) represent the the propagative modes whereas \square , \circ and \bullet represent the internal localized modes corresponding respectively to interstitial and cavity (with Dirichlet and Neumann conditions) modes. Moreover, ω_n/c (resp. ω_n^*/c) represent exact (resp. approximative) normalized eigenfrequencies.

ω_n/c	ω_n^*/c	Nature of modes	ω_n/c	ω_n^*/c	Nature of modes
2.1497	2.1487	\square	6.5190	6.6561	\cdot
2.5356	2.5431	\square	6.5847	6.5938	\square
2.9239	2.9259	\cdot	6.8852	6.8886	\cdot
3.0721	3.0906	\square	7.2871	7.3461	\square
3.6902	3.7242	\square	7.9267	8.3174	\cdot
4.2225	4.2901	\cdot	8.0781	8.0821	\square
4.4087	4.4070	\square	8.0886	8.1046	\bullet
5.0784	5.1192	\square	8.3332	8.4380	\cdot
5.7837	5.8503	\square	8.7357	9.0014	\cdot
5.8533	5.8567	\cdot	8.7811	8.8679	\square
6.2776	6.3202	\circ	9.0322	9.0374	\cdot
6.3391	6.3202	\circ			

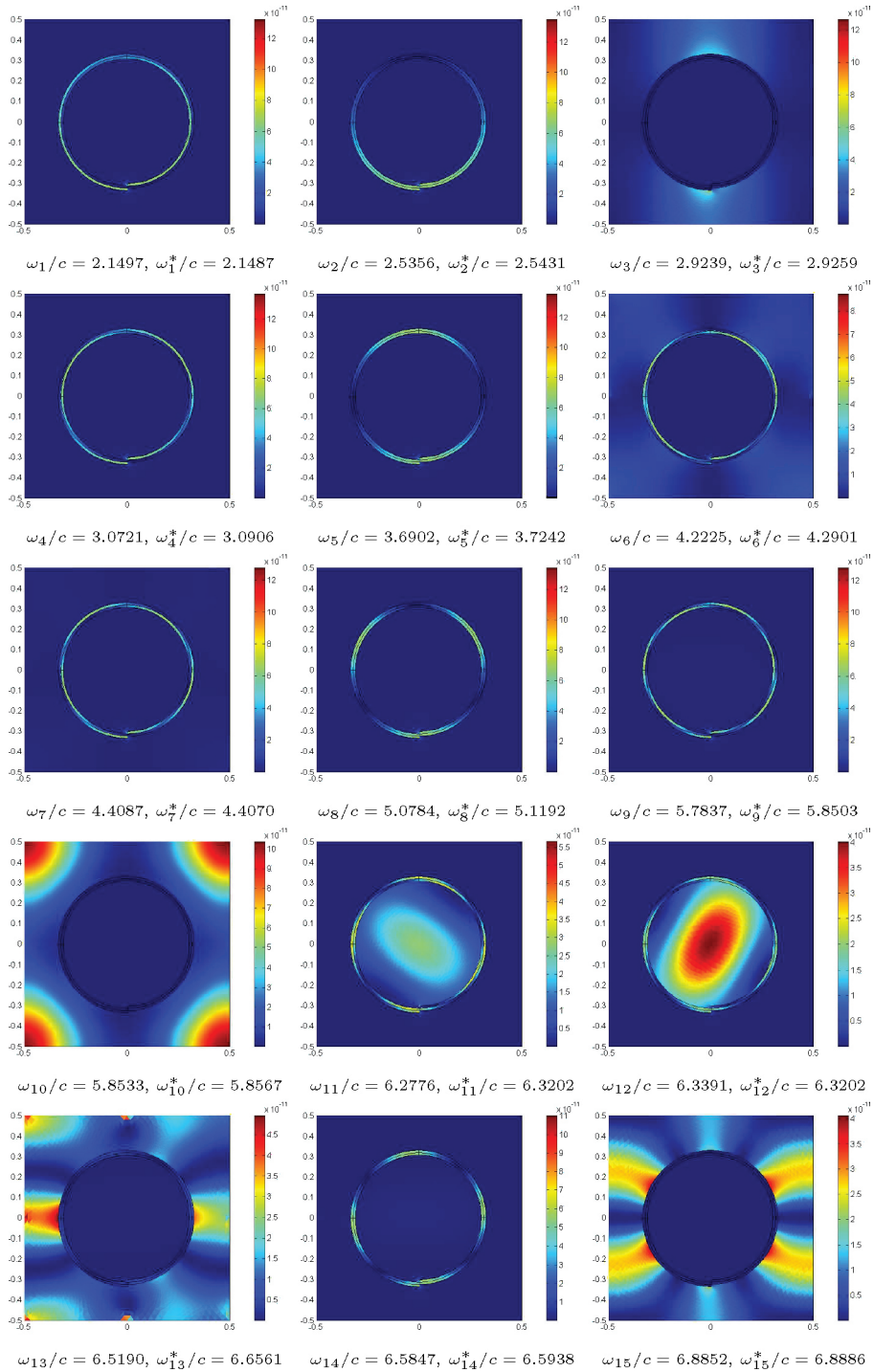


Figure 7. Maps of the total electromagnetic energy density of the first 15 modes together with their exact (resp. approximated) normalized eigenfrequencies ω_n/c (resp. ω_n^*/c) (see table 1).

which leads to resonant normalized eigenfrequencies:

$$k'_{0,n,m} = \sqrt{(\beta^2 + \kappa_{n,m}^2) / \varepsilon'_r}.$$

Figure 6 and table 1 show that the approximation is relevant even for high frequencies ($\frac{\omega}{c} \approx 10$).

6. Parametrizable Swill rolls: Dressed dispersion curves

As explained in the previous paragraph, the band diagram associated with the Swiss rolls can be seen as the juxtaposition of a ‘classical’ band diagram associated with propagating modes and flat curves associated with internal localized modes. Besides, it is worth noting that, for a given β , the eigenfrequencies associated with interstitial modes only depend on L and this length is independent of the external size of the Swiss roll. If, for any reason, an eigenfrequency $k_{0,1} = \sqrt{(\beta^2 + \frac{\pi^2}{L^2}) / \varepsilon_r}$ is required, several loops are necessary for a small Swiss roll whereas a quarter of loop may be sufficient for a Swiss roll which almost entirely fills the basic cell of the lattice. As a result, a classical band diagram can be dressed *ad libitum* by an independent band diagram associated with localized modes. By way of example, figures 7 and 8 show various maps of eigenfields for a large and a small Swiss roll. The distinction between localized and propagative modes is manifest. As claimed above, note, in figure 8, that the interstitial mode associated with the twelfth mode which lies within the interstices

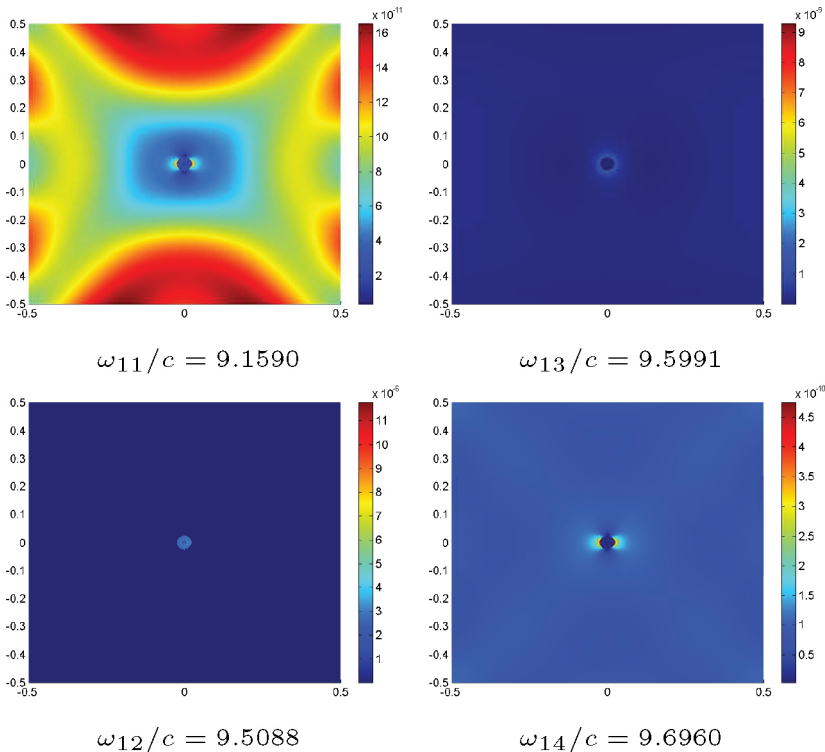


Figure 8. Four consecutive different modes associated with a small sextuple loop Swiss roll corresponding to the point X .

corresponds to a pretty small eigenfrequency $\omega_{12}/c = 9.5088$. This fairly surprising result is due to the six loops of the Swiss roll in question.

7. Conclusion

Optical and microwave metamaterials are expected to allow the development of innovative devices. The versatility of the finite element method allows a fast and easy exploration of the properties of such composite materials involving quite complicated geometries.

In the case of the Swiss roll lattice, for instance, it gives hints to fully explain the physical behavior of the structure. The metallic cylinder lattice has a large forbidden gap where the localized modes of the rolls can lie. The rolled structure gives a large equivalent length that allows us to reach frequencies that are low enough to lie inside the gap. The obtained flat curves correspond to null transverse group velocity that guarantees the extreme anisotropy of this material required by some applications [2].

References

- [1] Zolla, F., Renversez, G., Nicolet, A., Khulmey, B., Guenneau, S. and Felbacq, D., 2005, *Foundations of Photonic Crystal Fibres* (London: Imperial College Press).
- [2] Wiltshire, M.C.K., Hajnal, J.V., Pendry, J.B. and Edwards, D.J., 2003, Near field imaging with magnetic wires. *Optics Express*, **11**, 709–715.
- [3] Nicolet, A., Guenneau, S., Geuzaine, C. and Zolla, F., 2004, Modelling of electromagnetic waves in periodic media with finite elements. *Journal of Computational and Applied Mathematics*, **168**, 321–329.
- [4] Guenneau, S., Geuzaine, C., Nicolet, A., Movchan, A.B. and Zolla, F., 2004, Low frequency electromagnetic waves in periodic structures. *International Journal of Applied Electromagnetics and Mechanics*, **19**, 479–483.
- [5] Guenneau, S., Nicolet, A., Geuzaine, C., Zolla, F. and Movchan, A.B., 2005, Comparison of finite element and Rayleigh methods for the study of conical Bloch waves in arrays of metallic cylinders. *The International Journal for Computation and Mathematics in Electrical and Electronic Engineering*, **23**, No. 4., 932–949.